Supporting information for: Periodically-Ordered One and Two Dimensional CdTe QD Superstructures: A Path Forward in Photovoltaics

Moumita Kar,[†] Biplab Rajbanshi,[†,¶] Ritabrata Sarkar,[‡] Sougata Pal,[‡] and Pranab Sarkar[*,†]

Department of Chemistry, Visva-Bharati University, Santiniketan- 731235, *India, and Department of Chemistry, University of Gour Banga, Malda-* 732103, *India*

E-mail: pranab.sarkar@visva-bharati.ac.in

---

[*] To whom correspondence should be addressed

[†] Visva-Bharati University

[‡] Gour Banga University

[¶] Present address: Department of Chemical Engineering, University of South Carolina, 301 South Main Street, Columbia, South Carolina 29208, United States

Supporting Information

1. Details of SCC-DFTB method.
2. HOMO and LUMO charge densities of ester linked 1D linear superstructures containing different number of QDs of different sizes.
3. HOMO and LUMO charge densities of ester linked 2D hexagonal and square ordered superstructures containing different number of QDs.
4. Absorbance spectra of ester linked 1D linear assembled QD containing different number of CdTe QDs.
5. Band gap values of ester linked 1D linear, 2D hexagonal and square ordered superstructures containing different number of QDs of different sizes.
6. Charge densities plots of HOMOs and LUMOs of amide linked 1D linear assembled structures of CdTe QDs.
7. Optimized structures of amide linked assembly when the amide linkage are not orderly aligned.
8. HOMO and LUMO charge densities of amide linked 2D hexagonal and square ordered superstructures containing different number of QDs.
9. The HOMO and LUMO energy levels and band gap values of different sized QD are compared with previous experimental results.
10. Excitation energy, oscillator strength, involved molecular orbitals of different transitions of assembled QD.
11. Dipole moment values of assembled QD where amide linkage are orderly and not orderly aligned.

Details of SCC-DFTB method:

In SCC-DFTB method, the total energy can be expressed as a second order expansion of the density-functional theory (DFT) Kohn-Sham[1,2] total energy with respect to charge density fluctuations:[3]

$$E_{total}^{DFTB} = \sum_{i}^{occ} n_i \langle \Psi_i | \hat{H}_0 | \Psi_i \rangle + \frac{1}{2} \sum_{\alpha\beta}^{N} \gamma_{\alpha\beta} \Delta q_\alpha \Delta q_\beta + \sum_{\alpha<\beta} V_{\alpha\beta}^{rep} \tag{1}$$

The first term of Eq. (1) is the sum over all the occupied eigenfunctions Ψ_i of the effective Kohn-Sham Hamiltonian $\hat{H}_0$ which is derived under the approximation that the initial electronic density of the many-electron system can be represented as a superposition of corresponding neutral atomic charge densities (n_0). The second term is the energy contribution caused by density fluctuations (deviations from the reference atomic charge densities). The analytical interpolating function, $\gamma_{\alpha\beta}$ (α, β indexes denote the atoms) is dependent on Hubbard parameter (U) which is determined from the first derivative of the total atomic energy with respect to the electronic occupation around the neutral-atom electronic density.[3] Final term is the repulsion energy between two atoms which is obtained from the difference between the SCC-DFTB electronic energy (sum of first and second term of Eq. (1)) and the total DFT energy for some reasonably chosen reference system.

In DFTB method, only the valence electrons are explicitly considered and the inner electrons are treated within the frozen core approximation. The single particle Kohn-Sham eigen functions Ψ_i are constructed as a linear combination of atomic orbitals:

$$\Psi_i = \sum_n c_n \Phi_n \tag{2}$$

The functions Φ_n, expanded as a linear combination of Slater-type orbitals (STOs), obtained by self-consistent DFT based calculations with Perdew-Burke-Ernzerhof (PBE) exchange-correlation functional,[4] in the presence of additional confining harmonic potential $(\frac{r}{r_0})^2$ used to localize the atomic orbitals in the atomic Kohn-Sham equations.[3] Having defined the atomic orbitals (Φ), the atomic charge fluctuations (Δq) and Hubbard parameter are estimated. Then the DFTB electronic energy is calculated self-consistently by following the secular equation:[3]

$$\sum_n c_{in}(H_{nm} - \varepsilon_i S_{nm}) = 0; \forall m, i \tag{3}$$

with $H_{nm} = H^0_{nm} + \frac{1}{2} S_{nm} \sum_{\eta}^{N} (\gamma_{\alpha\eta} + \gamma_{\beta\eta}) \Delta q_\eta$ and $H^0_{nm} = \langle \Phi_n | \hat{H}_0 | \Phi_m \rangle$, $S_{nm} = \langle \Phi_n | \Phi_m \rangle$; $\forall n \in \alpha, m \in \beta$. Next the atom-atom repulsion energy is calculated from the difference of DFT total energy and the electronic DFTB energy as we have already mentioned earlier. Therefore, the necessary parameters for SCC-DFTB method are the Hamiltonian (H^0_{nm}) and overlap (S_{nm}) matrix elements, Hubbard parameters for every chemical element and the pairwise repulsive potentials for all interacting neighbors. The above parameters are calculated once and stored in so-called Slater-Koster files. The goodness of SCC-DFTB parametrization implies how it well reproduce the results with DFT or experiment. These parameters are later used in SCC-DFTB method.

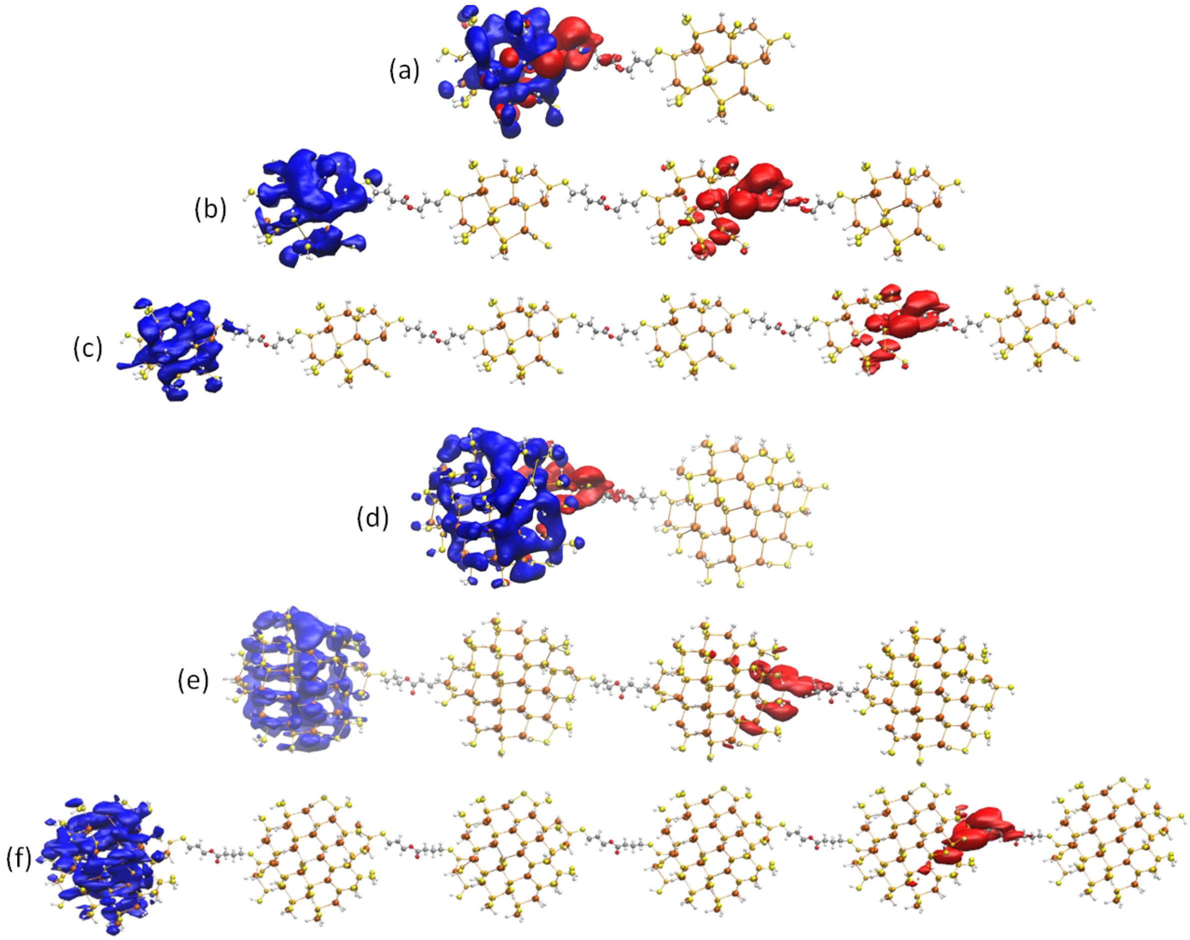

Figure S1: HOMO and LUMO charge densities of ester linked 1D linear assembled QD containing different number of $Cd_{17}Te_{17}$ [(a)-(c)] and $Cd_{65}Te_{65}$ [(d)-(f)] QDs. The red surface represents the HOMO, whereas blue surface represents the LUMO.

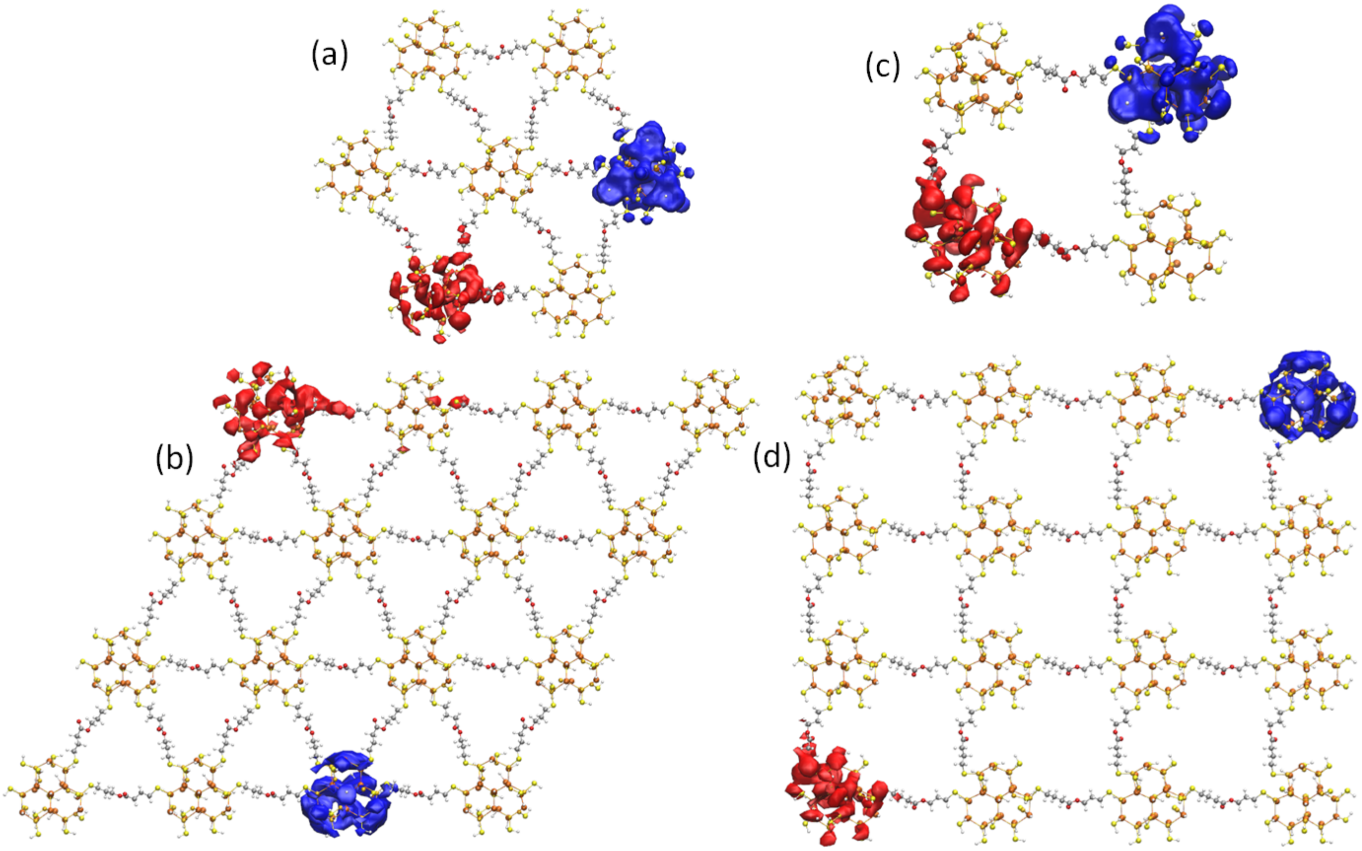

Figure S2: HOMO and LUMO charge densities of ester linked 2D hexagonal [(a), (b)] and square [(c), (d)] ordered assembled $Cd_{17}Te_{17}$ QD containing different number of QDs. The red surface represents the HOMO, whereas blue surface represents the LUMO.

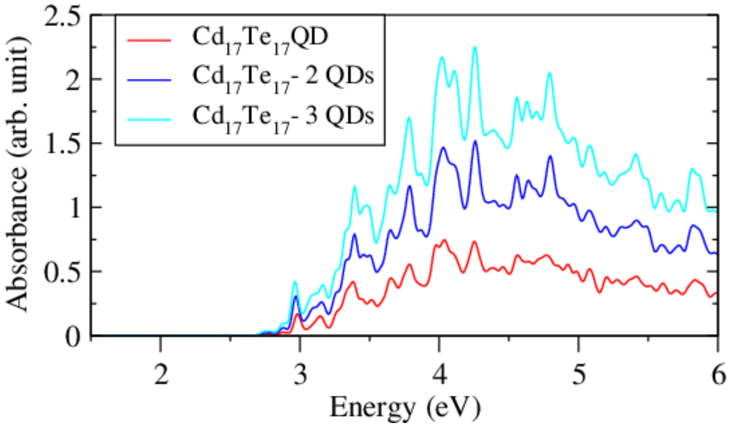

Figure S3: Absorbance spectra of single $Cd_{17}Te_{17}QD$ and its ester linked 1D linear assembly containing different number of QDs.

Table S1: The calculated band gap (E_g in eV) of single Cd_nTe_n QD (n=17, 34, 65, 98) and ester linked 1D linear superstructures containing different number of QDs. N denotes the number of QD(s).

QD(s)	($Cd_{17}Te_{17}$) E_g (eV)	($Cd_{34}Te_{34}$) E_g (eV)	($Cd_{65}Te_{65}$) E_g (eV)	($Cd_{98}Te_{98}$) E_g (eV)
N=1	2.74	2.50	2.06	1.84
N=2	2.46	2.18	1.79	1.65
N=3	2.45	2.16	1.72	1.64
N=4	2.45	2.16	1.71	1.64
N=5	2.45	2.16	1.70	1.62
N=6	2.45	2.15	1.70	1.64

Table S2: The calculated band gap (E_g in eV) of ester linked 2D hexagonal and square ordered superstructures containing different number of Cd_nTe_n QDs (n=17). N denotes the number of QDs.

QD		E_g
$Cd_{17}Te_{17}$	2D-hexagonal:N=7	2.22
	N=16	2.21
$Cd_{17}Te_{17}$	2D-square:N=4	2.21
	N=16	2.20

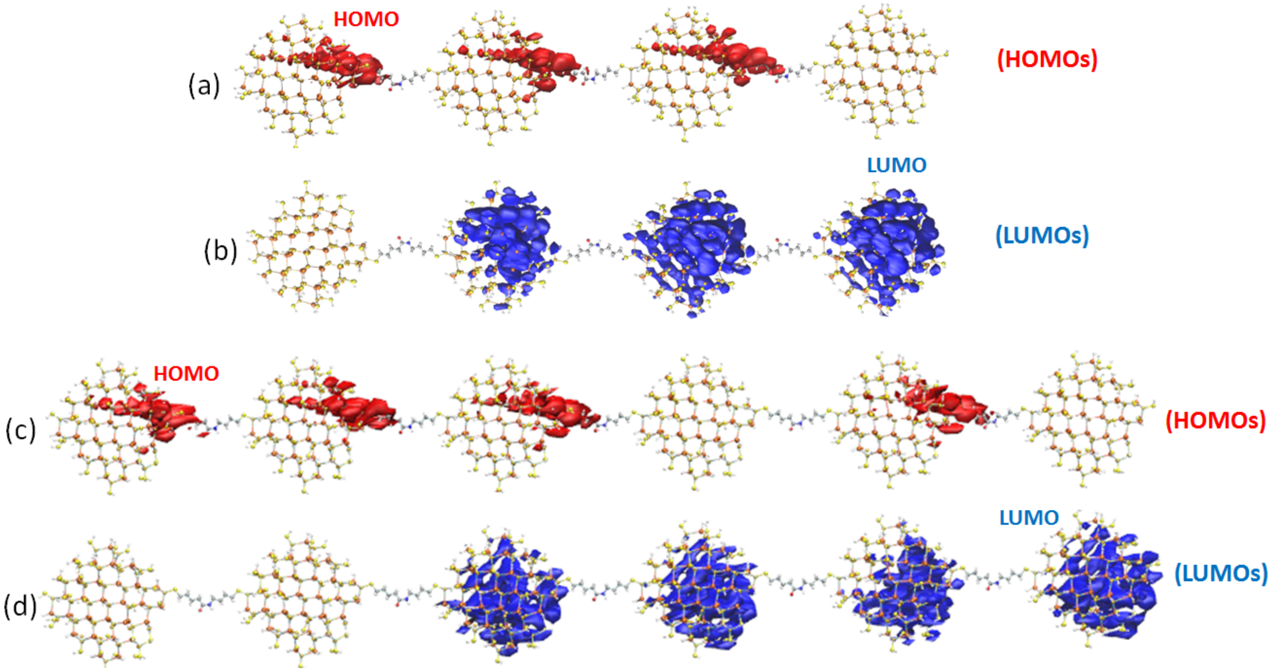

Figure S4: HOMOs and LUMOs localized on subsequent QDs in amide linked 1D linear assembled structures having [(a)-(b)] four $Cd_{98}Te_{98}$ QDs and [(c)-(d)] six $Cd_{98}Te_{98}$ QDs. The red surface represents the HOMOs, whereas blue surface represents the LUMOs.

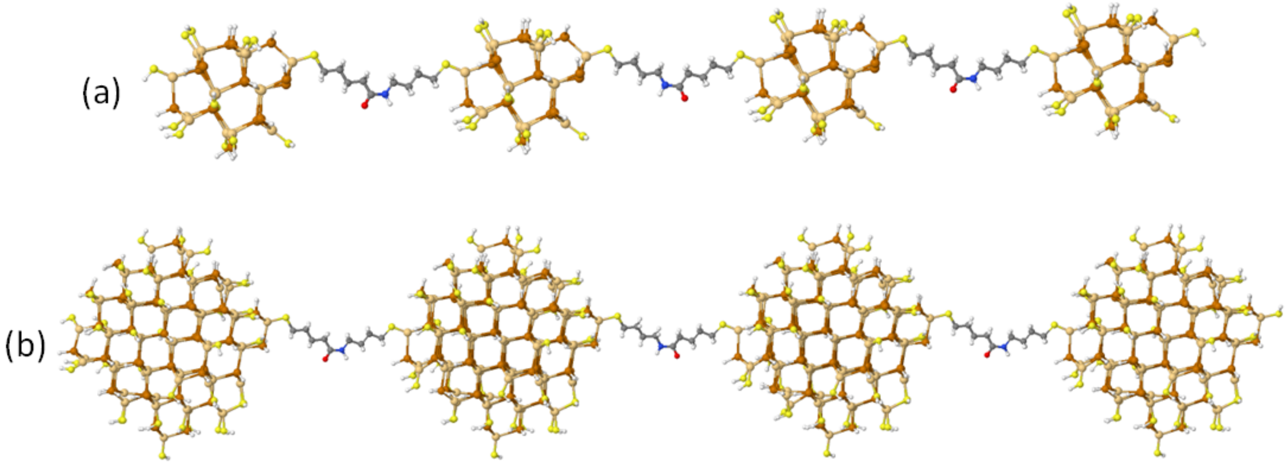

Figure S5: Optimized structures of amide linked assembly when the amide linkage are not orderly aligned. (a) $Cd_{17}Te_{17}$ QD assembly; (b)$Cd_{98}Te_{98}$ QD assembly.

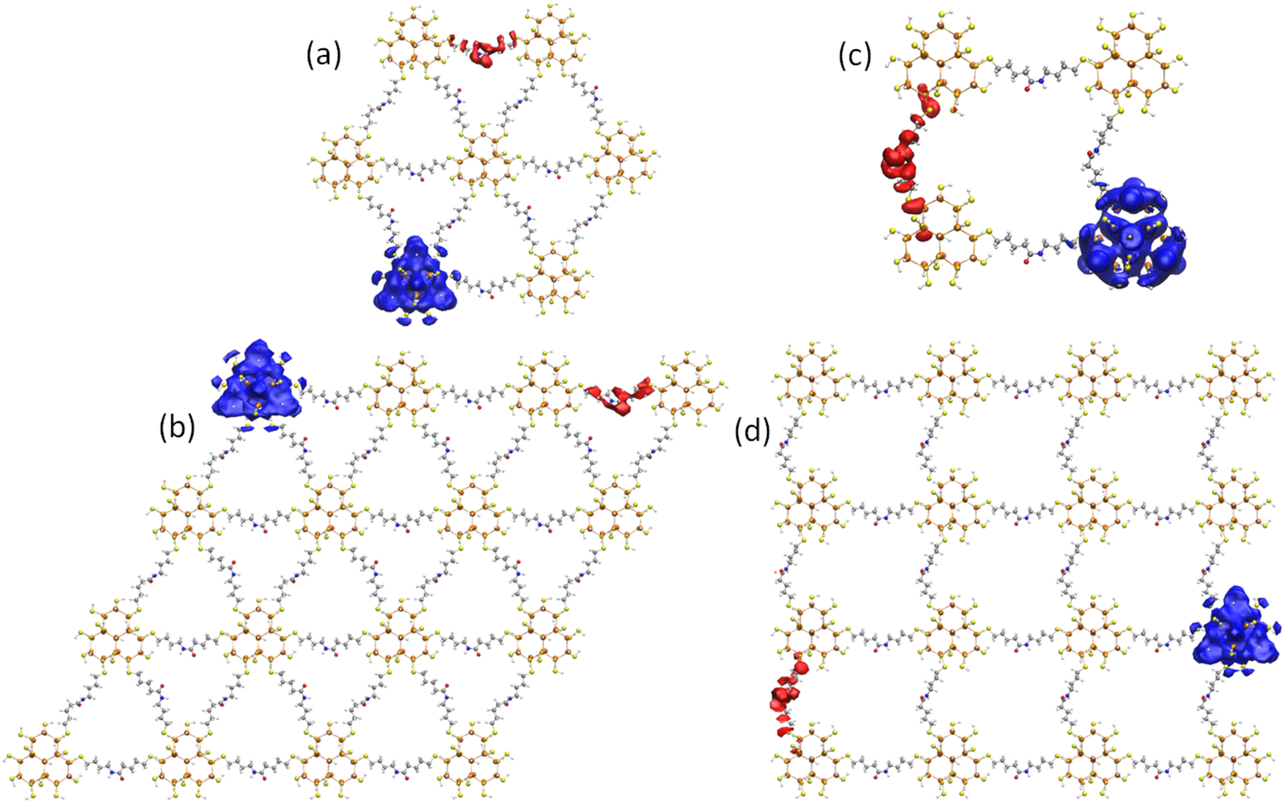

Figure S6: HOMO and LUMO charge densities of amide linked 2D hexagonal [(a), (b)] and square [(c), (d)] ordered $Cd_{17}Te_{17}$ QD structures containing different number of QDs. The red surface represents the HOMO, whereas blue surface represents the LUMO.

Table S3: The HOMO and LUMO energy levels and band gap values of different sized QD. These values are compared with the experimental values from UV-vis spectroscopy and cyclic voltammetry.[5]

our result				from UV-vis spectroscopy		from cyclic voltammetry			
QD-size diameter (nm)	HOMO-level (eV)	LUMO-level (eV)	HOMO-LUMO gap (eV)	QD-size diameter (nm)	optical band gap (eV)	QD-size diameter (nm)	HOMO-level (eV)	LUMO-level (eV)	gap (eV)
1.82	-5.94	-3.20	2.74	2.4	2.40	2.4	-6.02	-3.61	2.41
2.16	-5.54	-3.04	2.50	2.8	2.33	2.8	-5.88	-3.53	2.34
2.56	-5.29	-3.23	2.06	3.1	2.19	3.1	-5.76	-3.57	2.19
2.90	-5.38	-3.54	1.84						

Table S4: Transition energies (E, in eV), oscillator strength (f) and involved molecular orbitals of $Cd_{17}Te_{17}$ QD assembly (containing two QDs). H stand for HOMO and L stand for LUMO.

States	E (in eV)	f	involved orbitals
S_1	2.332	0.0000015	H -> L
S_2	2.387	0.0002266	H -> L+1
S_3	2.401	0.0000010	H-1 -> L
S_4	2.457	0.0005348	H-1 -> L+1
S_5	2.486	0.0002230	H -> L+2
S_6	2.555	0.0000061	H -> L+3
S_7	2.555	0.0000010	H-1 -> L+2
S_8	2.580	0.0000198	H -> L+4
S_9	2.581	0.0000001	H -> L+5
S_{10}	2.600	0.0000112	H -> L+6
S_{11}	2.624	0.0000000	H-1 -> L+3
S_{12}	2.626	0.0000652	H -> L+7
S_{13}	2.648	0.0000672	H -> L+8
S_{14}	2.649	0.0000010	H-1 -> L+4
S_{15}	2.651	0.0000131	H-1 -> L+5
S_{16}	2.669	0.0000000	H-1 -> L+6
S_{17}	2.679	0.0001381	H -> L+9
S_{18}	2.695	0.0000042	H -> L+10
S_{19}	2.697	0.0009026	H-1 -> L+7
S_{20}	2.713	0.0000010	H-2 -> L
S_{21}	2.721	0.0026699	H-1 -> L+8
S_{22}	2.722	0.0000001	H -> L+11
S_{23}	2.730	0.0000010	H-3 -> L
S_{24}	2.750	0.0001934	H-1 -> L+9
S_{25}	2.751	0.0017162	H-4 -> L
S_{26}	2.761	0.0000020	H -> L+12
S_{27}	2.765	0.0000000	H-1 -> L+10
S_{28}	2.771	0.0010221	H-2 -> L+1
S_{29}	2.785	0.0000306	H -> L+13
S_{30}	2.787	0.0014409	H-3 -> L+1
S_{31}	2.788	0.0000000	H-5 -> L
S_{32}	2.791	0.0000041	H -> L+14
S_{33}	2.792	0.0000000	H-1 -> L+11
S_{34}	2.803	0.0000000	H-4 -> L+1
S_{35}	2.805	0.0000000	H-6 -> L
S_{36}	2.808	0.0005521	H-7 -> L
S_{37}	2.812	0.0000032	H -> L+15
S_{38}	2.816	0.0000000	H-9 -> L
S_{39}	2.819	0.0013119	H-8 -> L
S_{40}	2.826	0.0000000	H-10 -> L

Table S5: Transition energies (E, in eV), oscillator strength (f) and involved molecular orbitals of $Cd_{17}Te_{17}$ QD assembly (containing three QDs). H stand for HOMO and L stand for LUMO.

States	E (in eV)	f	involved orbitals
S_1	2.304	0.0000010	H -> L
S_2	2.338	0.0000009	H-1 -> L
S_3	2.344	0.0000020	H -> L+1
S_4	2.378	0.0002320	H-1 -> L+1
S_5	2.379	0.0000010	H-2 -> L
S_6	2.382	0.0002396	H -> L+2
S_7	2.416	0.0000010	H-1 -> L+2
S_8	2.420	0.0000010	H-2 -> L+1
S_9	2.423	0.0000010	H-3 -> L
S_{10}	2.458	0.0005758	H-2 -> L+2
S_{11}	2.464	0.0005847	H-3 -> L+1
S_{12}	2.464	0.0000000	H -> L+3
S_{13}	2.498	0.0001932	H-1 -> L+3
S_{14}	2.499	0.0002111	H -> L+4
S_{15}	2.501	0.0000010	H-3 -> L+2
S_{16}	2.525	0.0000000	H -> L+5
S_{17}	2.533	0.0000003	H-1 -> L+4
S_{18}	2.539	0.0000000	H-2 -> L+3
S_{19}	2.545	0.0000000	H -> L+6
S_{20}	2.559	0.0000105	H-1 -> L+5
S_{21}	2.564	0.0000002	H -> L+7
S_{22}	2.570	0.0000000	H -> L+8
S_{23}	2.575	0.0000001	H-2 -> L+4
S_{24}	2.576	0.0000056	H -> L+9
S_{25}	2.579	0.0000257	H-1 -> L+6
S_{26}	2.583	0.0000000	H-3 -> L+3
S_{27}	2.596	0.0000310	H -> L+10
S_{28}	2.598	0.0000000	H-1 -> L+7
S_{29}	2.600	0.0000000	H-2 -> L+5
S_{30}	2.604	0.0000143	H-1 -> L+6
S_{31}	2.610	0.0001405	H-1 -> L+9
S_{32}	2.618	0.0000220	H-3 -> L+4
S_{33}	2.620	0.0000000	H-2 -> L+6
S_{34}	2.623	0.0000915	H -> L+11
S_{35}	2.627	0.0000081	H -> L+12
S_{36}	2.630	0.0000606	H-1 -> L+10
S_{37}	2.639	0.0000178	H-2 -> L+7
S_{38}	2.644	0.0000000	H-3 -> L+5
S_{39}	2.645	0.0000984	H -> L+13
S_{40}	2.645	0.0000000	H-2 -> L+8

Table S6: The calculated average dipole moment per QD (μ, in Debye) along the chain of amide linked $Cd_{17}Te_{17}$ QD assembly. N denotes the number of QDs in assembly. μ_1 : dipole moment of assembly when the amide linking between the QDs are orderly aligned (..-QD-CONH-QD-CONH-QD-CONH-QD-..); μ_2 : dipole moment of assembly when the amide linking between the QDs are not orderly aligned (..-QD-CONH-QD-NHCO-QD-CONH-QD-..).

No. of QDs	μ_1 (Debye)	μ_2 (Debye)
N= 3	3.04	0.24
N= 4	3.43	1.28
N= 5	3.71	0.28
N= 6	3.74	0.61

Table S7: The calculated average dipole moment per QD (μ, in Debye) along the chain of amide linked $Cd_{98}Te_{98}$ QD assembly. N denotes the number of QDs in assembly. μ_1 : dipole moment of assembly when the amide linking beween the QDs are orderly aligned (..-QD-CONH-QD-CONH-QD-CONH-QD-..); μ_2 : dipole moment of assembly when the amide linking between the QDs are not orderly aligned (..-QD-CONH-QD-NHCO-QD-CONH-QD-..).

No. of QDs	μ_1 (Debye)	μ_2 (Debye)
N= 3	11.78	8.1
N= 4	12.39	9.57
N= 5	14.04	8.0
N= 6	14.27	8.2

References

(1) Hohenberg, P.; Kohn, W. Inhomogeneous electron gas. *Phys. Rev. B* **1964**, *136*, 864.

(2) Kohn, W.; Sham, L. J. Self-consistent equations including exchange and correlation effects. *Phys. Rev. A* **1965**, *140*, 1133.

(3) Koskinen, P.; Mäkinen, V. Density-functional tight-binding for beginners. *Comput. Mater. Sci.* **2009**, *47*, 237–253.

(4) Perdew, J. P.; Burke, K.; Ernzerhof, M. Generalized gradient approximation made simple. *Phys. Rev. Lett.* **1996**, *77*, 3865.

(5) Haram, S. K.; Kshirsagar, A.; Gujarathi, Y. D.; Ingole, P. P.; Nene, O. A.; Markad, G. B.; Nanavati, S. P. Quantum confinement in CdTe quantum dots: Investigation through cyclic voltammetry supported by density functional theory (DFT). *J. Phys. Chem. C* **2011**, *115*, 6243–6249.